# Proximal sensing of penetration resistance at a permanent grassland site in Southern Finland

**Hella Ellen Ahrends[1], Antti Lajunen[1]**

[1]University of Helsinki, Department of Agricultural Sciences, Finland

**Abstract.**

*Proximal soil sensing allows for assessing soil spatial heterogeneity at a high spatial resolution. These data can be used for decision support on soil and crop agronomic management. Recent sensor systems are capable of simultaneously mapping several variables, such as soil electrical conductivity (EC), spectral reflectance, temperature, and water content, in real-time. In autumn 2021, we used a commercial soil scanner (Veris iScan+) to derive information on soil spatial variability for a permanent grassland field located at the Viikki Research Farm in Southern Finland. In this study, the relation between mapped soil layer data and multi-temporal soil resistance profile data derived from hand-held penetrometer measurements were explored. Mean soil resistance was negatively and positively related with topsoil moisture and EC data, but temporal changes in soil resistance were more closely related to reflectance in the Red and the IR region of the electromagnetic spectrum. Results from the test field illustrate the potential but also the limitations of using multi-sensor data platforms at permanent grassland sites, i.e. the influence of biomass on spectral reflectance during the peak growing season but also the potential of using data for tracking soil characteristics that result from multiple properties which dynamically change over time.*

**Keywords.**
*proximal soil scanning; soil spatial heterogeneity; electrical conductivity; soil penetration resistance.*

# Introduction

Proximal soil sensing devices aim to gain more knowledge on soil properties, their spatial variation and temporal dynamics using relatively simple and robust measurement and sensor techniques (Adamchuk et al. 2011). Signals detected from commonly applied sensors are, however, rather an integrative measure of multiple soil properties. Their interpretation is challenging due to the multiple uncertainty factors that vary in time and space. Uncertainty might be especially high at permanent grassland soils were living and dead biomass below and above the surface might affect measurements. On the other hand, uncalibrated data from such sites might be able to track seasonal changes in spatial patterns of highly dynamic soil characteristics such as soil water contents or soil resistance.

In Southern Finland, low altitude clay soils proximal to the sea can be influenced by water logging and are often used as permanent grassland. An important characteristic of such fields is their resistance which is linked to their vulnerability for compaction and to soil functions, such as carbon dioxide sequestration, gas exchange and biomass production. Resistance dynamically changes throughout the year and is strongly dependent on texture, soil water contents and vegetation cover as well as the work done by agricultural machinery.

The objective of the study is to explore the relation between raw proximal soil scanning data, that can be easily obtained at the soils surface, with soil penetration resistance metrics as well as seasonal changes in resistance. Scanning data (consisting of Apparent Electrical Conductivity (EC), raw Red and IR reflectance values, topsoil temperature and water content data) were obtained after the growing season in 2021 using a Veris iScan device (Veris Technologies, USA). Test field was a permanent grassland field located in Helsinki, Southern Finland. More specifically we aim to study if proximal soil scanning data in general and, more specifically, which scanning variables can identify (1) zones with significant differences in resistance metrics and (2) zones with strong seasonal dynamics in resistance metrics.

# Material and Methods

### Measurement site and data aquistion

The test field "Alaniitty1" is located at the Viikki Research Farm in Southern Finland (Helsinki) and measures 6.67 ha. The dominant texture of the topsoil is sandy clay (see Mokma et al. 2000 for a description of soil types in the area). Scanning data were obtained using a Veris iScan+ device after the growing season on September 10, 2021.

The iScan+ system simultaneously maps soil electrical conductivity, relative reflectance in the IR and the Red part of the electromagnetic spectrum (Red and IR values), soil water content and soil temperature (Kweon & Maxton 2013, Lund & Maxton 2019). The system is powered by a 12V outlet from the pulling vehicle. The system has an integrated GPS receiver, but this study used positioning data received using a separate GNSS receiver and RTK (Real Time Kinematic) correction signal. Apparent electrical conductivity measurements (EC) are based on galvanic contact measurements (EC up to a depth of ~60cm). The Optical Module consists of two LEDs emitting modulated (alternating) light pulses in the wavelengths 660 (Red) and 940 nm (Near Infrared) and a photodiode measuring reflected light (Kweon & Maxton 2013). Light is transmitted through a sapphire window which is pressed against the bottom of the furrow (~4−10 cm below the surface with a consistent pressure in order to support self-cleaning of the window). The signal is converted to DC voltage and digitized by a 12-bit A/D converter. Resulting data represent uncalibrated reflectance values, thus, "digital numbers" with a maximum reading of 4095. Topsoil moisture and temperature are measured with a capacitance sensor and a thermopile sensor, respectively. Further, based on the positioning data, topography data (height above mean sea level, slope and curvature) was obtained.

**Proceedings of the 15th International Conference on Precision Agriculture**
**June 26-29, 2022, Minneapolis, Minnesota, United States**

2

Based on a TARMO EURO tool adapter (Eurotool, Inc., USA), a sub-frame providing a 3-point linkage that allows for easily mounting the measurement device to any tractor, was constructed (Figure 1). Further, the system was equipped with adjustable wheels (SAMI supporting wheels, AS SAMI, Estonia). Data were recorded at a rate of 1Hz. For the test field a total number of 2935 scanning points were obtained. Data include control scans, thus, points from scan rows that traverse existing scan rows, to perform a quality control based on duplicated or nearby points. Duplicated values were removed prior to the analyses.



Fig 1. Veris iScan+ device, custom sub-frame for mounting the device and supporting wheels.

Soil resistance was measured at 10 points evenly distributed across the field using a hand-held penetrometer on four dates before (May 5th), during (June 16th and August 13th, subsequent to grass cuts) and after the growing season (October 21st) in 2021 using a hand-held penetrometer (Penetrologger, Eijkelkamp, Netherlands). The penetrometer was operated with 1 cm vertical resolution and at a speed of 4 cm s$^{-1}$ up to a depth of about 80 cm. Profiles represent average values of 4 replicates. The location of these measurement points is based on the preliminary definition of management zones (optimized for seeding rate) computed by the Veris FieldView software. Thereby field specific gradients in the sensor data are captured and spatial autocorrelation was avoided.

## Data processing and analyses

Outliers from raw point data (see Appendix, Fig. A1) were removed (points more than two standard deviations from the mean of the 10 neighboring points). Data were interpolated using median kernel smoothing to compute maps for each scanning variable. Soil resistance profiles were smoothed using locally weighted regression (LOESS function) and mean, minimum, maximum and the standard deviation (SD) of soil resistances were derived. Further, we estimated the depth of maximum resistance. The seasonal change of these values was computed by subtracting spring values (May 2021) from data obtained later during and after the growing season (with resulting positive values indicating higher resistance in spring/ higher depth to the layer with maximum resistance in spring).

For the 10 measurement locations we derived the average of the 10 nearest neighbors (features) from the interpolated scanning data and tested for significant correlations (Spearman rank correlation) with the corresponding soil resistance metrics. This is based on the assumption that field-specific gradients in both sensor and soil resistance data will lead to significant statistical relations. Further, the Welch Test was applied to test for significant differences in soil resistance profiles between the management zones suggested by the FieldView software.

**Proceedings of the 15th International Conference on Precision Agriculture**
**June 26-29, 2022, Minneapolis, Minnesota, United States**

3

# Results and Discussion

## Soil resistance metrics

Soil resistance increased in June after the start of the growing season (in especial for the topsoil layer) and was highest in August while it was similar to spring (May) measurements in October (Figure 2). Between 30 and 40cm there was a layer with maximum resistance. Exceptionally dry and warm summer season might have an influence on the harder surface resistances right after the summer in August.

Seasonal dynamics were most pronounced for profile 4 whereas they were lowest for profiles 3, 5 and 8 (except for August data). The latter profiles also showed strong vertical homogeneity (i.e., profile 6). According to the WelchTest in May profile 1 had higher and profiles 2 and 3 lower mean and maximum resistance values compared with most other profiles. Profile 7 showed a significantly higher coefficient of variation (CV). In June, profile 3 showed lower mean and maximum resistances compared to the other profiles and 10 a higher cv. In August, there were no significant differences but in October profile 3 had lower man and maximum resistances and profile 2 a higher cv compared to several other profiles.
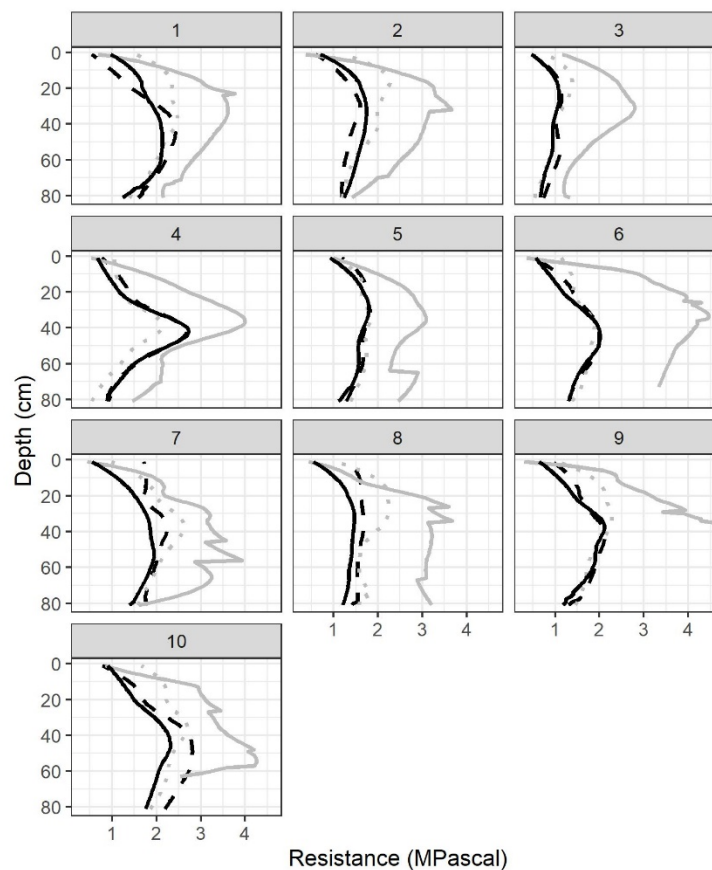


**Fig 2. Soil penetration resistance profiles obtained at 10 sampling points on May 04 (dashed black line), June 16 (dotted gray line), August 13 (solid gray line) and October 21 (solid black line).**

## Correlations between Veris data and resistance metrics

Mean soil resistance positively and negatively correlates with EC and topsoil moisture, respectively (Table 1). This indicates that soils which have a higher resistance had a higher electrical conductivity and lower topsoil moisture contents. Beside soil moisture, higher EC values are most probably related to higher clay contents and a higher Cation Exchange Capacity (CEC). Thus, topsoil moisture, followed by EC (both measured in autumn), was a suitable indicator for assessing spatial differences in the mean profile resistance. For EC correlations were highest in

**Proceedings of the 15th International Conference on Precision Agriculture**
**June 26-29, 2022, Minneapolis, Minnesota, United States**

4

June, thus, directly after the first grass cut (Table 1, Figure 3).

In August there was also negative relation between resistance and the normalized difference between IR and Red values (NIRR), indicating that during the period with maximum soil resistance and the peak vegetation season, the normalized difference between IR and Red decreases with decreasing resistance. This is related to the fact that in August IR showed a significant positive correlation with minimum resistance. With minimum values in August always being located in the first few centimeters of the soil (Figure 1) this indicates that soils where the resistance was very high in the uppermost layer, also had higher IR values. Based on a visual inspection of the bottom furrow we suggest that this results from the effect of dead and living (e.g., roots) biomass on IR values. In consequence, spectral data was biased by the presence of biomass.

**Table 1. Spearman rank correlation coefficients (cor) between Scanning variables (EC=Apparent Electrical conductivity, IR=Near Infrared vaues, Red=Red values, Mstr=Topsoil Moisture, NIRR=Normalized Difference IR-Red index, Slope=Slope, T=Topsoil Temperature) with soil minimum, maximum and mean soil resistance and the standard deviation (sd) of resistances for resistance measurements obtained on May 04, June 16, August 13 and October 21 in 2021 as well as the difference (diff) between dates (change in resistance over time).**

| Variable | resistance | cor | p-value | Temporal layer |
|---|---|---|---|---|
| EC | mean | 0.75 | 0.013 | 4-May |
| EC | minimum | 0.71 | 0.022 | 16-Jun |
| EC | maximum | 0.72 | 0.019 | 16-Jun |
| EC | mean | 0.82 | 0.004 | 16-Jun |
| EC | mean | 0.75 | 0.013 | 13-Aug |
| EC | mean | 0.73 | 0.016 | 21-Oct |
| EC | sd | 0.66 | 0.038 | diff. October-May |
| IR | minimum | 0.82 | 0.004 | 13-Aug |
| IR | maximum | -0.81 | 0.005 | diff. August-May |
| IR | sd | -0.78 | 0.008 | diff. August-May |
| Mstr | mean | -0.81 | 0.005 | 4-May |
| Mstr | mean | -0.77 | 0.009 | 16-Jun |
| Mstr | mean | -0.64 | 0.048 | 21-Oct |
| Mstr | sd | -0.67 | 0.033 | diff. October-May |
| Mstr | minimum | 0.79 | 0.006 | diff. October-May |
| NIRR | mean | -0.71 | 0.022 | 13-Aug |
| NIRR | maximum | -0.65 | 0.043 | 13-Aug |
| NIRR | minimum | 0.70 | 0.025 | diff. October-May |
| Red | minimum | 0.78 | 0.008 | 4-May |
| Red | mean | -0.84 | 0.002 | diff. October-May |
| Red | minimum | -0.65 | 0.043 | diff. October-May |
| Slope | sd | 0.77 | 0.009 | diff. June-May |
| T | minimum | 0.65 | 0.043 | 4-May |
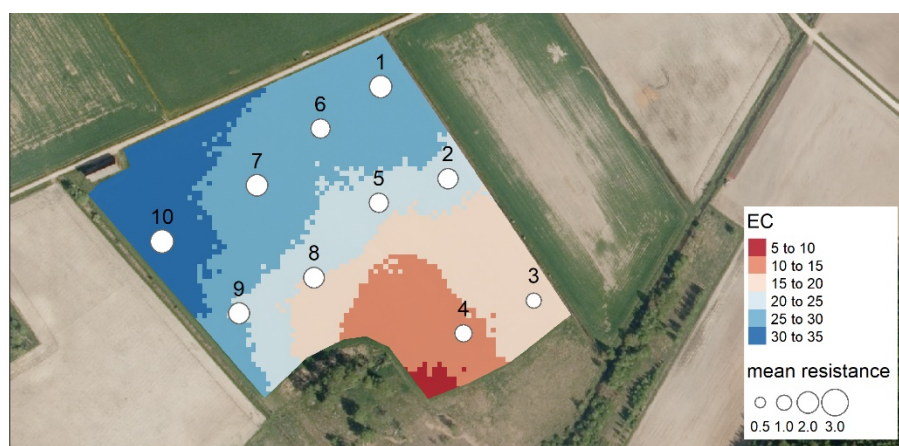


**Fig 3. Spatially interpolated EC values (September 21, 2021) and the mean soil penetration resistance observed on June 16 2021 (see Figure 1 for profile data).**

.

The change in soil resistance, obtained by subtracting resistance values measured in May from later observations (June, August and October), rather showed weak or non-significant

**Proceedings of the 15th International Conference on Precision Agriculture**
**June 26-29, 2022, Minneapolis, Minnesota, United States**

5

associations with autumn topsoil moisture and EC (Table 1). However, there was a negative relation between the change in the standard deviation (SD) and the maximum resistance from April to August with IR values, and a positive relation between the change in minimum resistance with the NIRR ratio. Differences in resistance metrics were always positive in August, thus, resistance was generally higher in summer compared with spring data. Correspondingly, the negative relation with IR values indicates that points where differences were high (suggesting more dynamics with strongly increased resistance in summer) showed lower reflectance values. The positive relation between the NIRR and change in minimum resistance indicates that points with higher dynamics (increased minimum resistance in summer) are further associated with an increased difference between NIR and Red values.

For the change in minimum and mean resistance between April and October there was a significant negative relation with Red values (Table 1, Figure 4). Differences were negative (Figure 5), thus, penetration resistance was either similar or lower after the growing season compared with May data. Correspondingly, the negative relation of differences with red values shows that points where minimum and mean resistances were comparatively more strongly decreased in October (higher values in April) showed comparatively higher Red values.

To understand and explain our observations, resistance data measured at higher spatial resolutions and multi-temporal scanning data are required. However, results suggest that the spatial variation in Red and NIR values might be associated with temporal dynamics in soil resistances. Increased Red and NIR reflectance values are commonly associated with higher contents of sand (brighter soil), lower soil water contents and lower contents of soil organic matter (Lobell & Asner 2002, Kusumo et al. 2009, 2010). Thus, the spectral signal is integrative for several soil characteristics that affect temporal dynamics of soil resistance at our test field (including topography effects). Integrating such spectral data with other data (e.g., topography) and combining it with points estimates of soil resistance might therefore allow for computing maps on the temporal dynamics of soil resistance at high spatial resolutions.
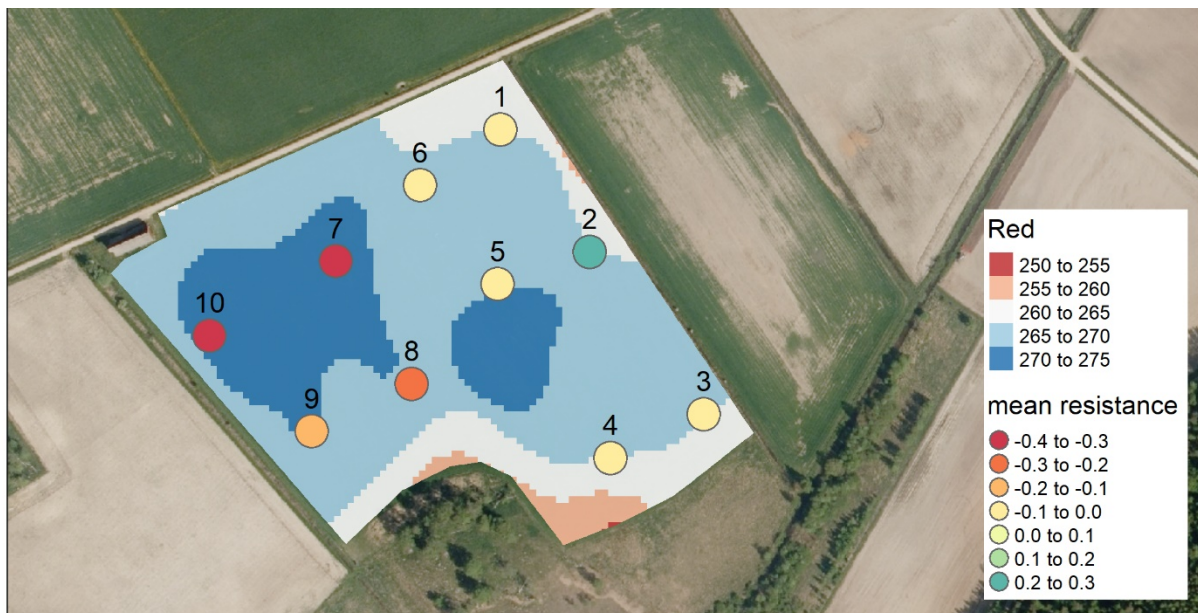


**Fig 4. Spatially interpolated Red values (September 21, 2021) and the change in the mean soil penetration resistance between April and October 21 (negative values indicating higher resistance in April).**

**Proceedings of the 15th International Conference on Precision Agriculture**
**June 26-29, 2022, Minneapolis, Minnesota, United States**

6
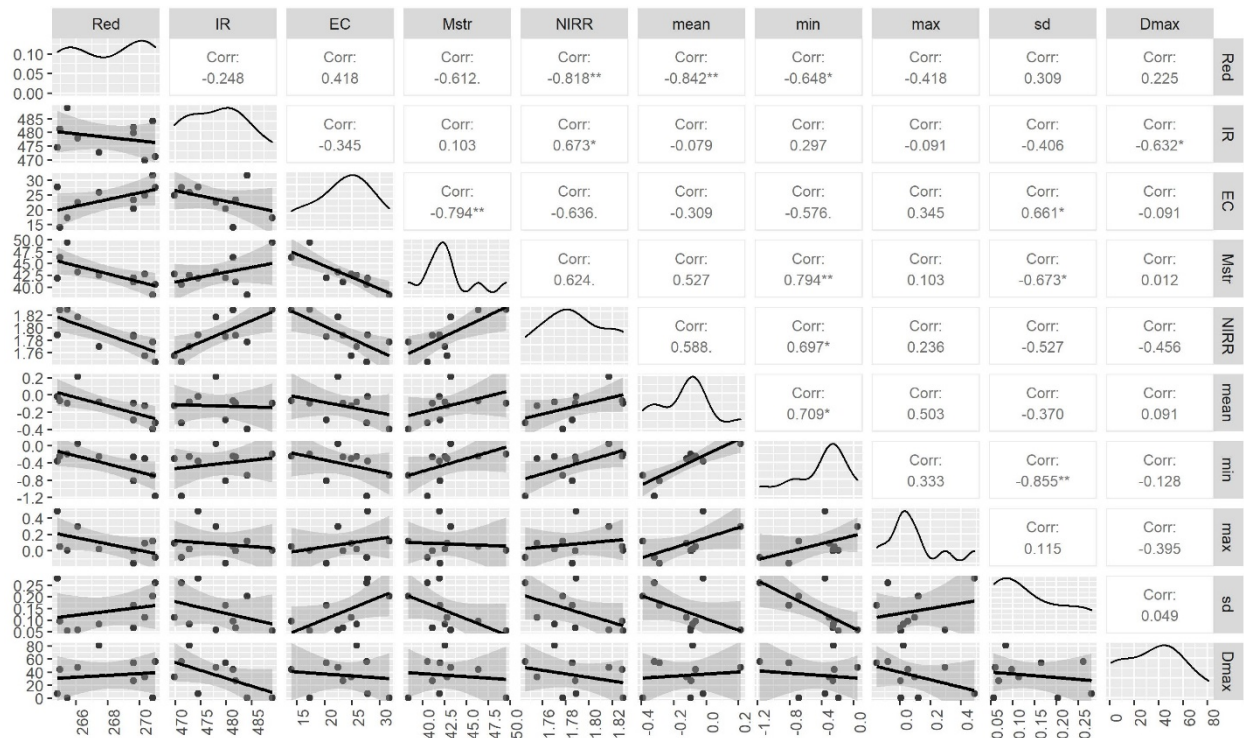
**Fig 5. Spearman rank correlations between scanned variables (September 21, 2021) and the difference in soil penetration resistance metrics between October and May 2021 (see Table 1 for abbreviations).**

## Summary and Conclusions

Uncalibrated proximal soil scanning data obtained at a permanent grassland field located in Southern Finland were related to summarized soil resistance metrics for exploring the relation between typical scanning variables that can be easily obtained at the soil surface with soil penetration resistance and the change in soil resistance over time. Apparent Electrical Conductivity and topsoil moisture obtained with a Veris iScan+ device showed significant statistical relations with mean resistances. However, temporal dynamics in resistance were rather related to spatial differences in IR and Red values. Results from this study will have to be verified with spatially more detailed observations of soil resistance and multi-temporal scanning data. However, they highlight both limitations and strengths of sensors used in proximal soil scanning studies by showing that 1) shank-based spectral data obtained at grassland sites might be biased by the presence of biomass, especially in the peak growing season and 2) the integrative nature of multi-sensor devices and scanning variables allows for relating measured data to soil characteristics such as resistance, that dynamically change over time.

### Acknowledgements

**Proceedings of the 15th International Conference on Precision Agriculture
June 26-29, 2022, Minneapolis, Minnesota, United States**

7

# References

Adamchuk, V.I. & Viscarra Rossel, R.A. (2011). Precision Agriculture: Proximal Soil Sensing. In: Encyclopedia of Agrophysics (eds. Gliński, J., Horabik, J. & Lipiec, J.). Springer Netherlands, Dordrecht, pp. 650–656. https://doi.org/ 10.1007/978-90-481-3585-1_126

Kusumo, B.H., Hedley, M.J., Hedley, C.B., Arnold, G.C. & Tuohy, M.P. (2010). Predicting pasture root density from soil spectral reflectance: field measurement. European Journal of Soil Science, 61, 1–13. https://doi.org/10.1111/j.1365-2389.2009.01199.x

Kusumo, B.H., Hedley, M.J., Hedley, C.B., Hueni, A., Arnold, G.C. & Tuohy, M.P. (2009). The use of Vis-NIR spectral reflectance for determining root density: evaluation of ryegrass roots in a glasshouse trial. European Journal of Soil Science, 60, 22–32. https://doi.org/10.1111/j.1365-2389.2008.01093.x

Kweon, G. & Maxton, C. (2013). Soil organic matter sensing with an on-the-go optical sensor. Biosystems Engineering, 115, 66–81. https://doi.org/10.1016/j.biosystemseng.2013.02.004

Lobell, D.B. & Asner, G.P. (2002). Moisture Effects on Soil Reflectance. Soil Science Society of America Journal, 66, 722–727. https://doi.org/10.2136/sssaj2002.7220

Lund, E. & Maxton, C. (2019). Comparing Organic Matter Estimations Using Two Farm Implement Mounted Proximal Sensing Technologies. In: PSS 2019. Presented at the 5th Global Workshop on Proximal Soil Sensing, Columbia, Missouri, USA, p. 35.

Mokma, D.L., Yli-Halla, M. & Hartikainen, H. (2000). Soils in a young landscape on the coast of southern Finland. AFSci, 9, 291–302. https://doi.org/10.23986/afsci.5670

# Appendix
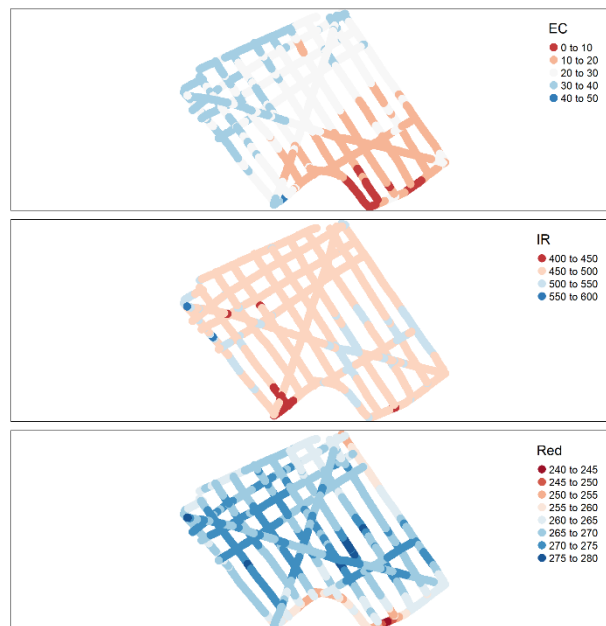


**Fig A1. Raw iScan point data for scanned variables: EC=apparent Electrical Conductivity (mS), Red=red reflectance (relative units/digital numbers), IR=near infrared reflectance (relative units/digital numbers), Scanning data obtained on September 21, 2021.**

**Proceedings of the 15th International Conference on Precision Agriculture**
**June 26-29, 2022, Minneapolis, Minnesota, United States**

8